

DOI: 10.1515/amm-2017-0219

H.P. KIM<sup>\*#</sup>, M.J. CHOI<sup>\*</sup>, S.W. KIM<sup>\*</sup>, D.J. KIM<sup>\*</sup>, Y.S. LIM<sup>\*</sup>, S.S. HWANG<sup>\*</sup>**EFFECTS OF GRAIN BOUNDARY MORPHOLOGIES ON STRESS CORROSION CRACKING OF ALLOY 600**

Effects of grain boundary morphologies on stress corrosion cracking (SCC) of Alloy 600 have been studied in 40% NaOH at 315°C using C-ring specimens. The configuration of the grain boundary and the intergranular carbide density were controlled by heat treatment. SCC tests were performed at +150 mV above the corrosion potential. The specimen with a serrated grain boundary showed higher SCC resistance than that with a straight grain boundary. This appears to be caused by the fact that the specimen with the serrated grain boundary has longer SCC path. SCC resistance also increased with intergranular carbide density probably due to enhanced relaxation of stress at intergranular carbide.

*Keywords:* Alloy 600, NaOH, stress corrosion cracking, grain boundary morphologies

**1. Introduction**

Since mill annealed Alloy 600 was used in the steam generator of nuclear power plants in the early 1970s, it experienced stress corrosion cracking (SCC) in both the primary coolant system and the secondary coolant system [1-7]. The degradation resulted in extended outage to repair and steam generator replacement, leading to significant economic loss. Thermally treated Alloy 600 was used in the late 1970s instead of mill annealed Alloy 600 because former is resistant to SCC [8-11]. However, the thermally treated Alloy 600 also underwent SCC in nuclear power plants. In response to the issue of SCC of mill annealed Alloy 600 and thermally treated Alloy 600, thermally treated Alloy 690 has been used as a steam tubing material in replaced steam generators and new nuclear power plants since 1989. The thermally treated Alloy 690 is almost immune to SCC in the primary coolant system, but it is more susceptible to SCC in highly caustic solutions with lead contaminants than Alloy 600. It is thus critically important to understand SCC behavior and to improve SCC resistance in caustic solutions. Recently, grain boundary engineering has been proposed to improve the creep resistance and/or SCC resistance for nickel base alloys [12-23]. Grain boundary engineering mainly focuses on grain boundary energy reduction and the formation of serrated grain boundary. The grain boundary energy reduction is usually achieved by introducing a high portion of coincidence site lattice boundary. Formation of serrated grain boundary is produced by special heat treatment. Nickel base alloys with a serrated grain boundary showed higher creep resistance, likely due to inhibition of grain boundary sliding. The serrated grain boundary can also be applied

to improve SCC resistance. Several mechanistic studies on the formation of a serrated grain boundary have been conducted. But there has been little work on the effect of the serrated grain boundary resistance to SCC of Alloy 600. In this work, the effect of a serrated grain boundary and grain boundary carbide density on SCC was studied with carefully controlled heat treatment to obtain a serrated grain boundary and a straight boundary and varying degree of intergranular carbide density, where the grain size of Alloy 600 was not changed substantially.

**2. Experimental Procedure**

The chemical composition of Alloy 600 used in this work is shown in Table 1. The heat treatment procedure is shown in Table 2. Heat treatment was performed to obtain a serrated boundary and a straight boundary, where the grain size of Alloy 600 was kept almost the same for both grain boundary morphologies by varying the solution heat treatment time and cooling rate. In addition, the degree of intergranular carbide density and grain boundary sensitization was respectively varied by additional heat treatment. Nitric acid etching was used to reveal the grain boundary structure and phosphoric acid to reveal chromium carbide.

TABLE 1

Chemical composition of Alloy 600

C	Cr	Ni	Fe	Si	Mn	S	Cu
0.04	15.4	75.1	8.0	0.1	0.3	<0.001	0.2

\* NUCLEAR MATERIALS SAFETY RESEARCH DIVISION, KOREA ATOMIC ENERGY RESEARCH INSTITUTE, 989-111 DAEDEOK-DAERO, YUSEONG-GU, DAEJEON, 305-353, REPUBLIC OF KOREA

# Corresponding author: hpkim@kaeri.re.kr

The C-ring specimen fabricated according to ASTM G38-73 was used for the SCC test. The 40% NaOH solution was prepared with demineralized water and reagent grade sodium hydroxide. It was purged with high purity nitrogen gas (99.9%) for 1 hour to deaerate the solution in a 3.8L Ni autoclave. The reference electrode and counter electrode were external Ag/AgCl and platinum wire, respectively. Potential was applied with an EG&G 263 potentiostat. The SCC test was performed at 315°C in 40% NaOH solution at potential of 150 mV above the open circuit potential. The SCC fracture surface was observed with an optical microscope and a scanning electron microscope.

### 3. Results and Discussion

#### 1) Effect of serrated grain boundary

Grain boundary structures with a serrated grain boundary and a straight grain boundary are shown in Fig. 1. Specimens

heat treated with either SA1+SERR or SA1+SERR+TT showed a serrated grain boundary. On the other hand, specimens heat treated with either SA2, SA2+SEN or SA2+TT showed a straight boundary. The chromium carbide distribution is shown in Fig. 2. The grain size of the specimens with a serrated boundary and a straight grain boundary was almost the same.

A serrated grain boundary was reported in nickel base and cobalt base super alloys and in some ceramic materials. A common feature of material with serrated grain boundary is that the precipitate and matrix has the same crystal structure and the lattice parameter of the precipitate is similar to or multiple times of that of the matrix [24]. Several mechanisms were proposed to explain serrated grain boundary formation. Tamazaki [25] proposed that precipitates are assumed to grow from one grain into the matrix of the adjacent grain and then the localized boundary displacement occurs to shorten the grain boundary length, finally thus forming a serrated grain boundary in austenitic stainless steel. Larson [26] suggested that the serrated grain boundary

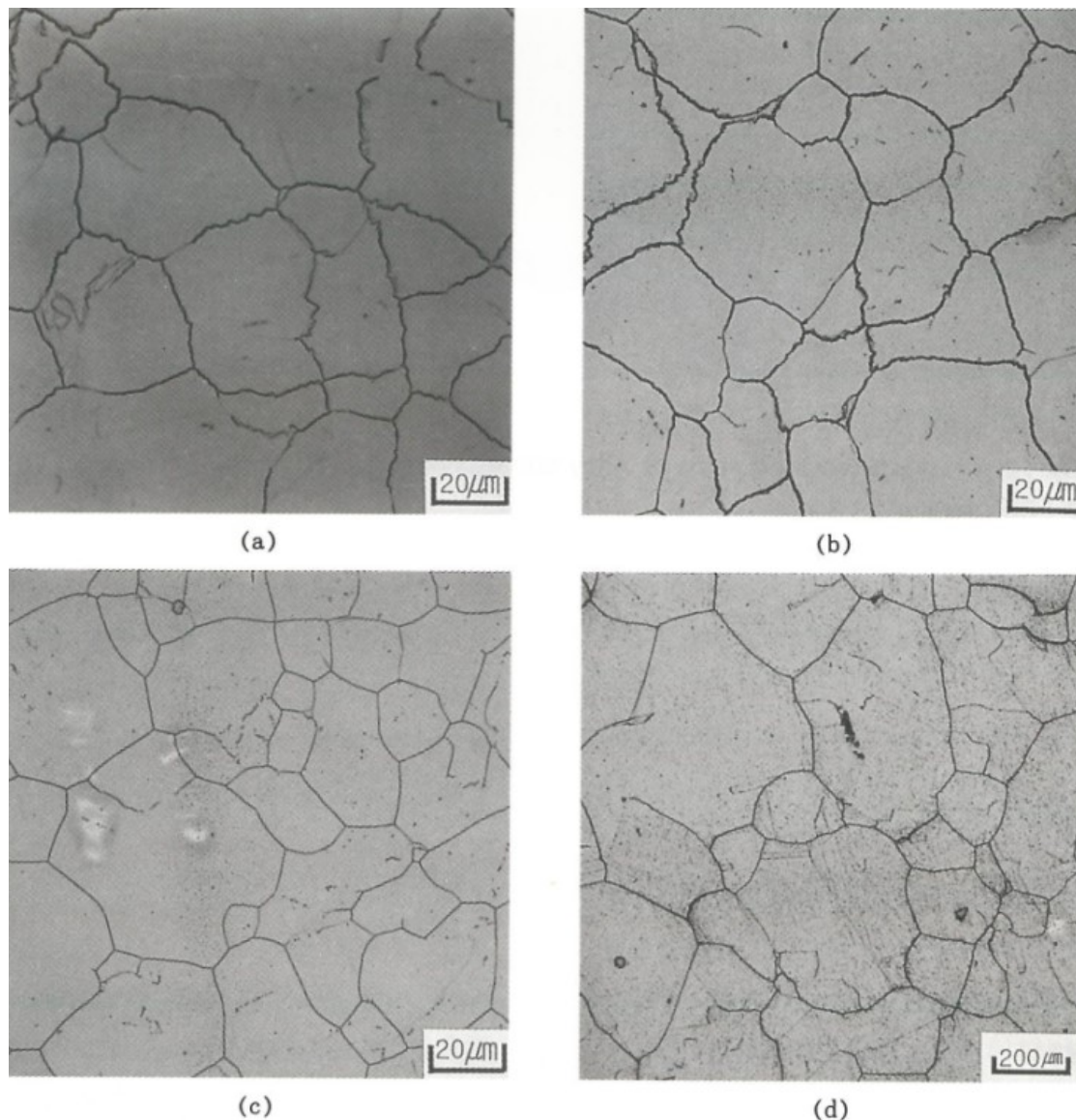


Fig. 1. SEM micrograph of grain boundary configuration of Alloy 600 etched in HNO<sub>3</sub>; (a) SA+SERR, (b) SA+SERR+TT, (c) SA+SEN and (d) SA+TT

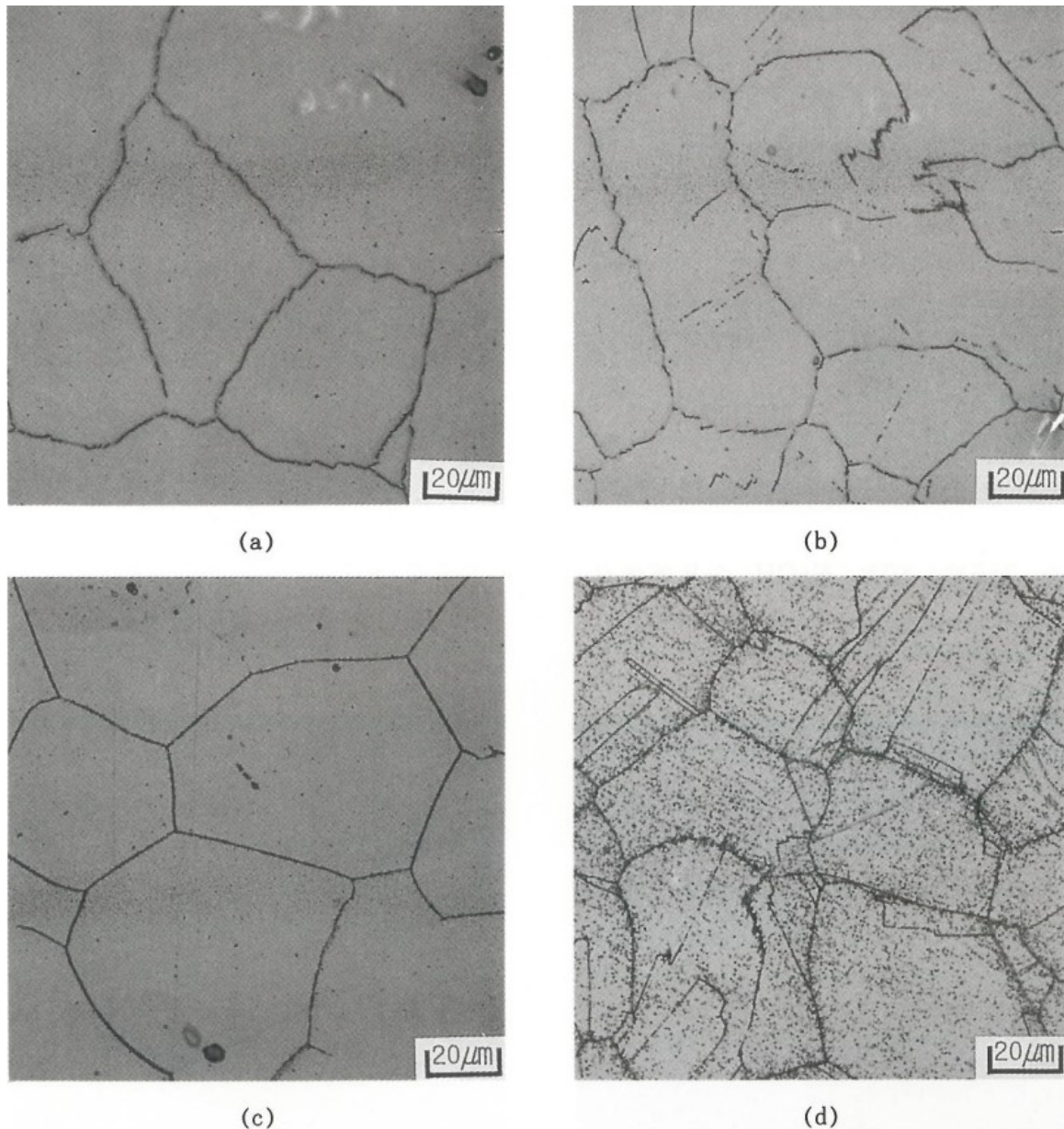


Fig. 2. SEM micrograph of chromium carbide of Alloy 600 etched in  $H_3PO_4$ ; (a) SA1+SERR, (b) SA1+SERR+TT, (c) SA2+SEN and (d) SA2+TT

formation is associated with the heterogeneous nucleation of  $\gamma'$  at the grain boundaries, and the migration of grain boundary sections between the primary  $\gamma'$  particles. Koul [27] proposed that the net strain energy difference between the matrix side and the boundary side of the particle matrix interface provided a driving force for the movement of primary  $\gamma'$  particles in the direction of the boundary. On the other hand, Yoo [24] suggested that the serrated grain boundary formation is related with asymmetric growth of precipitates.

Specimens with a serrated grain boundary showed higher SCC resistance compared to specimens with a straight grain boundary irrespective of intergranular carbide distribution. The SCC crack depth at the side of the C-ring specimen is shown in Fig. 3. The SCC depth was measured at the side of the C-ring specimen. The maximum SCC rate obtained by dividing the maximum depth at the side of the C-ring specimen with SCC

test duration is shown in Table 3. For the specimens with the serrated grain boundary, the specimen with SA1+SERR showed a more dense intergranular carbide distribution and higher SCC resistance than that with SA1+SERR+TT. Intergranular carbide in the SA1+SERR specimen may be coarsened during subsequent thermal treatment in the SA1+SERR+TT specimen. The SCC fracture surface for a specimen with a serrated grain boundary (Fig. 4a) showed a zigzag fracture surface, which is consistent with intergranular fracture of the serrated grain boundary. On the other hand, the SCC fracture surface for a specimen with a straight grain boundary (Fig. 4b) showed a smooth fracture surface, which is consistent with intergranular fracture of the straight grain boundary. The zigzag fracture surface for the serrated grain boundary means that the SCC path is longer in the serrated grain boundary than in the straight grain boundary.

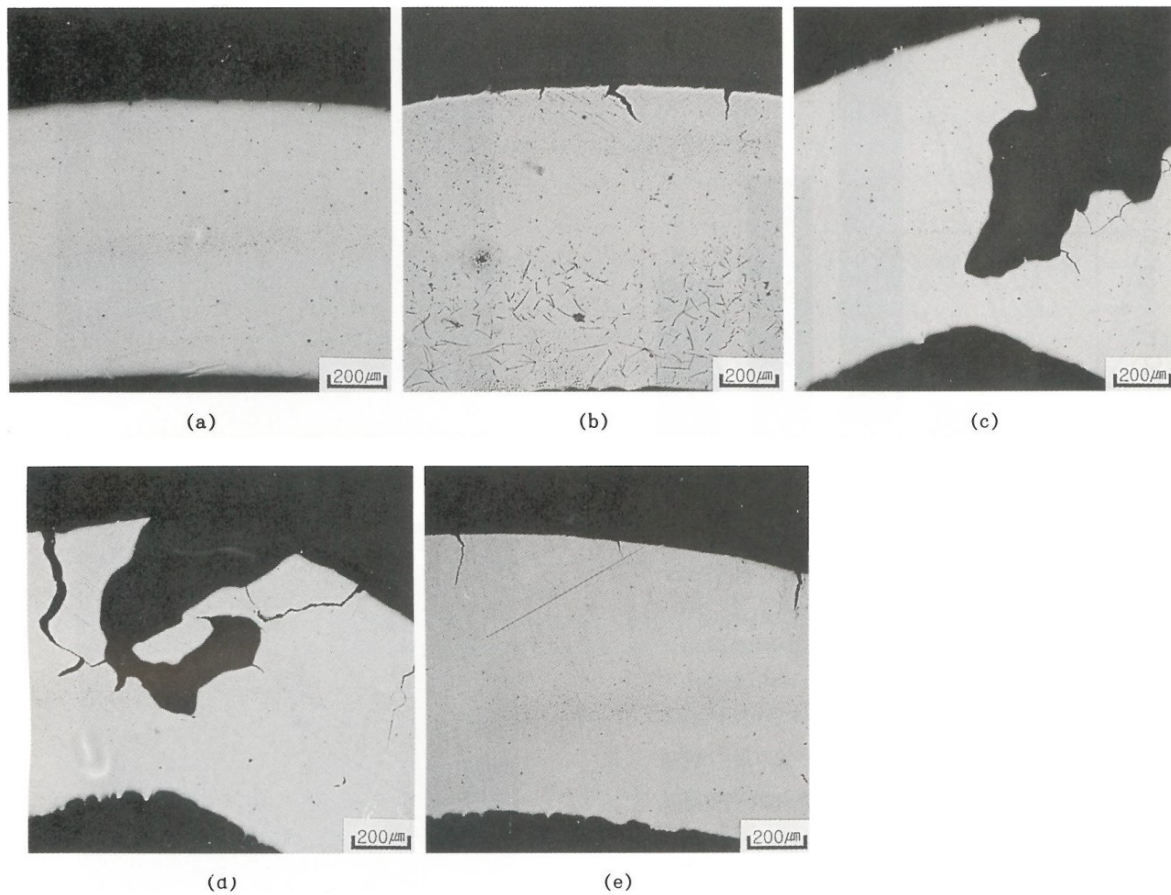


Fig. 3. Micrograph of crosssectional area of C-ring specimen showing stress corrosion cracks; (a) SA+SERR, (b) SA+SERR+TT, (c) SA, (d) SA+SEN, (e) SA+TT

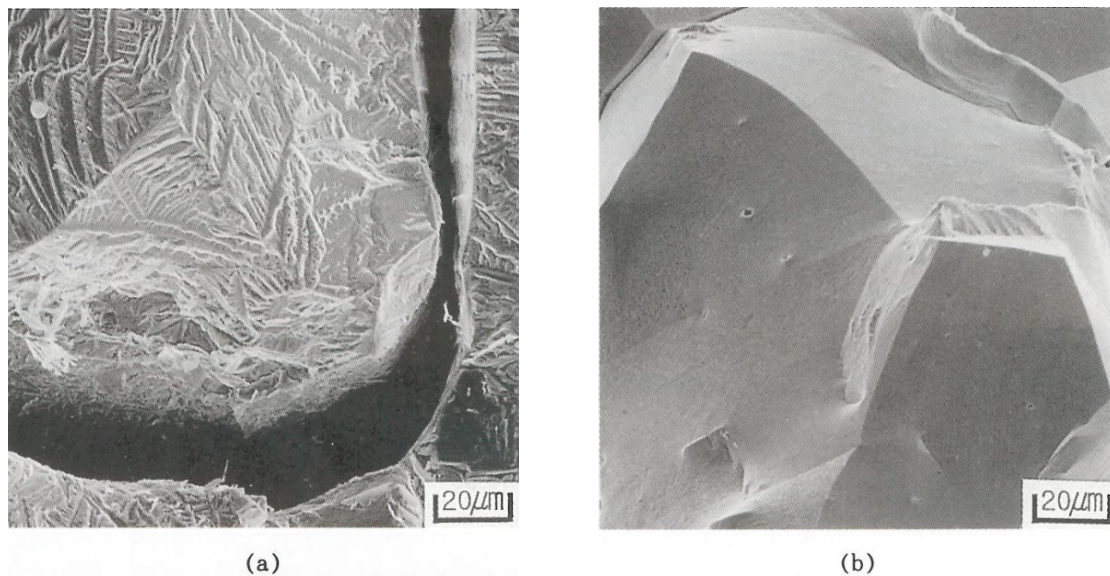


Fig. 4. SEM micrograph of stress corrosion cracking fracture surface; (a) serrated grain boundary, (b) straight grain boundary

## 2) Effect of intergranular carbide and chromium depletion at grain boundary

Alloy 600 was heat treated to SA2, SA2+SEN, and SA2+TT, as shown in Table 2, to determine the effect of intergranular carbide on SCC. The SA2, SA2+SEN, and SA2+TT specimens have similar grain size. Many works [28-31] showed that Cr content at

the grain boundary was lower in the SA2+SEN specimen than in SA2. Grain boundary chromium is accompanied by intergranular carbide precipitation. For the specimen of SA2+TT heat treated at higher temperature, Cr content at the grain boundary was partly recovered due to back diffusion of chromium from the matrix to the grain boundary. The SCC resistance increased in

TABLE 2

Heat treatment procedure of Alloy 600

Specimen designation	Heat treatment procedure
SA1-SERR	SA (1100°C/20 min) + slow cooling (1100°C~750°C, cooling rate: 0.3°C/min) + WQ
SA1-SERR-TT	SA (1100°C/20 min) + slow cooling (1100°C~750°C, cooling rate: 0.3°C/min) + WQ + TT (710°C/15 hrs) + WQ
SA2	SA(1100°C/30 min) + WQ
SA2-SEN	SA (1100°C/30 min) + WQ + SEN (600°C/24 hrs)
SA2-TT	SA (1100°C/30 min) + WQ + TT (710°C/15 hrs)

TABLE 3

Maximum stress corrosion crack propagation rate

Heat treatment	SA + SERR	SA1+SERR +TT	SA2	SA2+SEN	SA2+ TT
Max. SCC rate (mm/sec)	34.7	83.3	541.7	375	243.1

sequence of SA2, SA2+SEN and SA2+TT. The SCC resistance of sensitized specimen (SA2+SEN) was higher than that of solution annealed specimen (SA2), which is not consistent with the previous works in tetrathionate solution or thiosulfate solution [32-34]. Systematic study on the effect of bulk chromium content in solution annealed Ni-Cr-Fe alloy in a caustic solution also showed that the SCC resistance of Ni-Cr-Fe alloy increases with bulk chromium content [35]. The higher SCC resistance of SA2+SEN specimen compared with SA2 specimen may be attributed to highly caustic solution in this work. In highly caustic solution, beneficial effect of the intergranular carbide might be greater than harmful effect of chromium depletion. The beneficial effect of the intergranular carbide may be explained with the fact that the intergranular carbides promote crack blunting due to their effectiveness as a dislocation source [36]. The material which is resistant to SCC in specific environment may not be resistant to in the other environment, so careful consideration is needed in selecting material state for specific environment.

#### 4. Conclusion

Effects of grain boundary morphologies on stress corrosion cracking (SCC) of Alloy 600 have been studied in 40% NaOH at 315°C using C-ring specimens. The specimen with serrated grain boundary showed higher SCC resistance than that with straight grain boundary, likely due to the longer SCC path in serrated grain boundary. SCC resistance also increased with intergranular carbide density, probably due to enhanced relaxation of stress at intergranular carbide.

#### Acknowledgements

This work was supported by the National Research Foundation of Korea (NRF) Grant funded by the Korea government (MSIP).

#### REFERENCES

- [1] H.R. Copson, W.E. Berry, *Corrosion* **16**, 79 (1960).
- [2] H.R. Copson, W.E. Berry, *Corrosion* **18**, 21 (1962).
- [3] J.W. McGrew, *Corrosion* **18**, 27 (1962).
- [4] S.H. Bush, R.L. Dillon, International Conference on Stress Corrosion Cracking and Hydrogen Embrittlement of Iron Base Alloys, Firminy, France (1973).
- [5] D. van Rooyen, *Corrosion* **31**, 327 (1975).
- [6] J. Blanchet, H. Coriou, L. Grall, C. Mahieu, C. Otter, G. Turluer, *J. of Nuclear Materials* **55**, 187 (1975).
- [7] H.A. Domian, R.H. Emanuelson, L.W. Sarver, G.J. Theus, L. Katz, *Corrosion* **33**, 26 (1977).
- [8] T.S. Bulischek, D. van Rooyen, *Corrosion* **37**, 597 (1981).
- [9] G.P. Airey, EPRI-1354, 1980.
- [10] J.R. Crum, *Corrosion* **38**, 39 (1982).
- [11] R. Bandy, R. Robergy, D. van Rooyen, EPRI NP\_4458, A10-1 (1988).
- [12] T. Watanabe, *Res Mechanica* **11**, 47 (1984).
- [13] G. Palumbo, K.T. Aust, *Recrystallization* **90**, 101 (1990).
- [14] A. Roy, U. Erb, H. Gleiter, *Acta Metall.* **30**, 1847 (1982).
- [15] M. Yamashita, M. Yoshioka, T. Mimaka, S. Hashimoto, S. Miura, *Acta Metall.* **38**, 1619 (1990).
- [16] G.S. Crawford, G.S. Was, *Met. Trans A* **23A**, 1195 (1992).
- [17] G. Palumbo, P.J. King, K.T. Aust, U. Erb, P.C. Lichtenberger, *Scripta Met.* **25**, 1775 (1991).
- [18] P. Lin, G. Palumbo, U. Erb, K.T. Aust, *Scripta Met.* **33**, 1387 (1995).
- [19] T. Watanabe, Seminar presented in KAERI (1997).
- [20] H. Iizuka, M. Tanaka, *J. of Materials Science* **21**, 2803 (1986).
- [21] M. Tanaka, H. Iizuka, F. Ashihara, *J. of Materials Science* **23**, 3827 (1988).
- [22] M. Tanaka, H. Iizuka, F. Ashihara, *J. of Materials Science* **24**, 1623 (1989).
- [23] M. Tanaka, *J. of Materials Science* **27**, 4717 (1992).
- [24] Y.S. Yoo, Ph. D Thesis, KAIST (1992).
- [25] M. Tamazaki, *J. Japan Inst. Metals.* **30**, 1032 (1966).
- [26] J.M. Larson, *Met. Trans. A*, **7A**, 1497 (1976).
- [27] A.K. Koul, G.H. Gessinger, *Acta Metall.* **31**, 1061 (1983).
- [28] R. Bandy, R. Roberge, R.C. Newman, *Corrosion Science* **23**, 9, 995 (1983).
- [29] M.F. Maday, A. Mignone, M. Vittori, *Corrosion Science* **28** 9, 887 (1988).
- [30] W.-T. Tsai, M.-J. Sheu, J.-T. Lee, *Corrosion Science* **38**, 1, 3345 (1996).
- [31] J.J. Kai, C.H. Tsai, G.P. Yu, *Nuclear Engineering and Design* **144**, 449 (1993).
- [32] Newsletter on Three Mile Island Unit 1, *Nuclear News* **25**, 47 (1982).
- [33] H.S. Isaacs, B. Vyas, M.W. Kendig, *Corrosion* **38**, 130 (1982).
- [34] S. Dhawale, G. Cragolino, D.D. Macdonald, EPRI Report No. RP 1166-1, Electric Power Research Institute, Palo Alto (1982).
- [35] H.P. Kim, S.S. Hwang, Y.S. Lim, I.H. Kuk, J.S. Kim, *Metals and Materials International* **7**, 1, 55 (2001).
- [36] S.S. Hwang, Y.S. Lim, S.W. Kim, D.J. Kim, H.P. Kim, *Nuclear Engineering and Technology* **45**, 1, 73 (2013).